Enhanced Drought Exposure Increasingly Threatens More Forests Than Observed

Chongyang Xu, Hongyan Liu, Philippe Ciais, Henrik Hartmann, Jesús J Camarero, Xiuchen Wu, William M Hammond, Craig D Allen, Fahu Chen

▶ **To cite this version:**

Chongyang Xu, Hongyan Liu, Philippe Ciais, Henrik Hartmann, Jesús J Camarero, et al.. Enhanced Drought Exposure Increasingly Threatens More Forests Than Observed. Earth's Future, 2024, 12 (1), 10.1029/2023ef003705 . hal-04387951

HAL Id: hal-04387951
https://hal.science/hal-04387951

Submitted on 11 Jan 2024

HAL is a multi-disciplinary open access archive for the deposit and dissemination of scientific research documents, whether they are published or not. The documents may come from teaching and research institutions in France or abroad, or from public or private research centers.

L'archive ouverte pluridisciplinaire **HAL**, est destinée au dépôt et à la diffusion de documents scientifiques de niveau recherche, publiés ou non, émanant des établissements d'enseignement et de recherche français ou étrangers, des laboratoires publics ou privés.

Check for updates

Earth's Future

RESEARCH ARTICLE
10.1029/2023EF003705

Enhanced Drought Exposure Increasingly Threatens More Forests Than Observed

Chongyang Xu[1], Hongyan Liu[1], Philippe Ciais[2], Henrik Hartmann[3,4], Jesús J. Camarero[5], Xiuchen Wu[6], William M. Hammond[7], Craig D. Allen[8], and Fahu Chen[9,10,11]

[1]College of Urban and Environmental Sciences and Institute of Carbon Neutrality, Peking University, Beijing, China, [2]IPSL—LSCE, CEA CNRS UVSQ UPSaclay, Centre d'Etudes Orme des Merisiers, Gif sur Yvette, France, [3]Institute for Forest Protection, Julius Kühn Institute Federal Research Centre for Cultivated Plants, Quedlinburg, Germany, [4]Department of Biogeochemical Processes, Max Planck Institute for Biogeochemistry, Jena, Germany, [5]Instituto Pirenaico de Ecología (IPE-CSIC), Zaragoza, Spain, [6]State Key Laboratory of Earth Surface Processes and Resource Ecology, Beijing Normal University, Beijing, China, [7]Agronomy Department, University of Florida, Gainesville, FL, USA, [8]Department of Geography and Environmental Studies, University of New Mexico, Albuquerque, NM, USA, [9]Key Laboratory of Western China's Environmental Systems (Ministry of Education), College of Earth and Environmental Science, Center for Pan Third Pole Environment (Pan-TPE), Lanzhou University, Lanzhou, China, [10]Key Laboratory of Alpine Ecology (LAE), Institute of Tibetan Plateau Research, Chinese Academy of Sciences (CAS), Beijing, China, [11]CAS Center for Excellence in Tibetan Plateau Earth Sciences, Chinese Academy of Sciences (CAS), Beijing, China

Key Points:

- Forest mortality risk increased with drought exposure (DE) in both pulse and press droughts
- Rising CO_2 alleviated the increase of mortality risk with pulse drought, but it has little effect on that in press droughts
- DE threatened 0.28 billion hectares of global forested areas in the past decades and has been increasing in particular regions

Supporting Information:

Supporting Information may be found in the online version of this article.

Correspondence to:

H. Liu,
lhy@urban.pku.edu.cn

Citation:

Xu, C., Liu, H., Ciais, P., Hartmann, H., Camarero, J. J., Wu, X., et al. (2024). Enhanced drought exposure increasingly threatens more forests than observed. *Earth's Future*, *12*, e2023EF003705. https://doi.org/10.1029/2023EF003705

Received 7 APR 2023
Accepted 20 DEC 2023

Author Contributions:

Conceptualization: Chongyang Xu, Hongyan Liu
Data curation: Chongyang Xu
Formal analysis: Chongyang Xu
Funding acquisition: Chongyang Xu, Hongyan Liu
Investigation: Chongyang Xu
Methodology: Chongyang Xu
Project Administration: Chongyang Xu, Hongyan Liu
Resources: Chongyang Xu
Software: Chongyang Xu
Supervision: Hongyan Liu
Validation: Chongyang Xu
Visualization: Chongyang Xu
Writing – original draft: Chongyang Xu

© 2024 The Authors.
This is an open access article under the terms of the Creative Commons Attribution-NonCommercial License, which permits use, distribution and reproduction in any medium, provided the original work is properly cited and is not used for commercial purposes.

Abstract Forest protection and afforestation have been identified as a means to partially offset anthropogenic CO_2 emissions. Yet, increasingly frequent observations of drought-induced tree mortality are reported. Here, we applied a risk analysis framework for global drought-induced forest mortality by examining extreme reductions in greenness and water content of forest canopies during past mortality events as well as growth recovery of surviving individual trees following stand-scale mortality events. We defined a drought-induced mortality risk index (DMR) that explains 80% of documented tree mortality. Rising CO_2 alleviated the increase of DMR with short-term drought, however, the observed DMR increases with long-term drought no matter whether considering plant responses to CO_2. DMR in sites where tree mortality has been observed significantly increased since the 1980s. More than that, drought exposure threatened 0.28 billion hectares of forested areas. Our framework highlights how climate change-induced drought, especially hotter-droughts, threatens the sustainability of global forests.

Plain Language Summary Planting trees remains one of the most effective strategies for mitigating climate change. Studies suggest that an additional 900 million hectares of new tree-planted areas could be supported by current climate conditions. However, the benefits of massive forestation efforts may be offset by increasing drought-induced mortality. We conducted a risk analysis based on the robust relationship between forest mortality and drought. Our findings show that drought-induced mortality risk can identify 80.0% of documented tree mortality events. While rising CO_2 levels can alleviate the increase of mortality risk in short-term droughts, it has little effect on mortality risk during long-term droughts. In the past decades, both short- and long-term droughts have threatened 0.28 billion hectares of forested areas globally, and the mortality risk has been increasing in particular regions.

1. Introduction

Forests sequester up to 25% of anthropogenic carbon dioxide emissions annually, thus mitigating climate change (Bonan, 2008). However, the future of forests is highly uncertain (Brodribb et al., 2020), because most forested biomes are exposed to rising temperatures, atmospheric water demand and increasingly frequent and serve drought stress events (Allen et al., 2015). Sequestering atmospheric carbon comes at a cost for trees—for each molecule of carbon gained, many molecules of water are lost. During extended and intense drought and heat stress, this can lead to hydraulic dysfunction and ultimately to tree mortality (so called "hydraulic failure" (McDowell et al., 2008)), potentially causing large-scale tree dieback globally (Allen et al., 2015; Hammond et al., 2022). Currently, it remains unclear whether drought-induced mortality observations in many forested regions and biomes are representative of a general forest decline globally, and whether such a trend may continue given that more frequent, longer and more intense droughts are likely to occur with land surface warming (Ault, 2020; Liu et al., 2018; Touma et al., 2015).

Writing – review & editing: Chongyang Xu, Hongyan Liu, Philippe Ciais, Henrik Hartmann, Jesús J. Camarero, Xiuchen Wu, William M. Hammond, Craig D. Allen, Fahu Chen

A global synthesis of lethal drought experiments has shown that hydraulic failure is a mechanism ubiquitously associated with tree mortality (Adams et al., 2017), yet, simulation of mortality based on these results may overestimate individual-scale physiological stress and landscape-scale mortality rates in forest ecosystems (Fisher et al., 2018). Extreme drought events are generally considered as key drivers of extensive forest mortality (Allen et al., 2015), however, long-term stress of gradually drying climate may also decrease the ability of trees to recover from droughts and in turn amplify forest mortality induced by extreme droughts even further (Allen et al., 2015; Anderegg et al., 2020; Bauman et al., 2022; Matusick et al., 2018). To account for the interaction of extreme drought events (pulse drought) and progressive long-term drying (press drought), we applied a "press and pulse" framework inspired from description of disturbances in ecological systems (Harris et al., 2018) (Figure 1a) and analyzed historical forest mortality events based on the processes related to tree mortality or forest die-off, including canopy dieback and subsequent growth releases of surviving trees recorded in annual growth rings (Figure 1b). We addressed the following questions: (a) whether both pulse and press droughts increased tree mortality risk? (b) where were the hotspots of forest mortality in the past several decades?

2. Material and Methods

2.1. Data Sources

2.1.1. Drought Indices

We employed both meteorological drought indices and ecological drought indices to assess the extent of drought stress in our study. Palmer Drought Severity Index (PDSI, Osborn et al., 2018) and the Standardized Precipitatio n-Evapotranspiration Index (SPEI, Vicente-Serrano et al., 2010) are widely recognized as meteorological drought indices, which gauge the deviation in surface water balance by evaluating the disparity between precipitation and potential evapotranspiration (Dai, 2011; Vicente-Serrano et al., 2010). Monthly grids of the PDSI were obtained for 1901–2017 with 0.5° spatial resolution from the Climatic Research Unit at the University of East Anglia (http://www.cru.uea.ac.uk/). Considering that the PDSI has a fixed temporal scale, we used the SPEI calculated at a 3-month time scale (SPEI03) to consider the multiscalar nature of droughts (Vicente-Serrano et al., 2010). SPEI3 data with a spatial resolution of 0.5° were obtained from the IPE-CSIC (Zaragoza, Spain) SPEI database V2.4 (http://sac.csic.es/spei/database.html).

However, relying solely on meteorological drought indices may lead to an overestimation of the impact of drought, as elevated CO_2 levels can mitigate drought stress by enhancing water use efficiency (Swann et al., 2016), ultimately lowering the risk of forest mortality (Liu et al., 2017). Meanwhile, this process reduces vegetation transpiration and consumption of soil moisture (Yang et al., 2019). Therefore, we incorporate soil moisture as an additional drought stress indicator, which offer a more accurate reflection of the drought stress experienced by vegetation, taking into account in the potential reduced transpiration caused by the physiological response of plants to increasing CO_2 (Swann et al., 2016). In this study, we acquired monthly soil moisture grids for the period 1980–2017, with a spatial resolution of 0.25°, from the Global Land Evaporation Amsterdam Model (GLEAM) outputs (https://www.gleam.eu/). GLEAM soil moisture data was assimilated from diverse data sets, including satellite-based observations of soil moisture and vegetation optical depth (VOD) (Martens et al., 2017). To address the limitations of GLEAM soil moisture data, which features a restricted temporal coverage and may not align optimally with tree-ring data, we supplemented our analysis with soil moisture data from the Global Land Data Assimilation System (GLDAS, https://ldas.gsfc.nasa.gov/gldas). Models in the GLDAS project used satellite-based leaf area index products as vegetation parameters to generate land surface fluxes (Rodell et al., 2004). The GLDAS soil moisture data covers the period from 1948 to 2014, with a spatial resolution of 0.25°. Soil moisture data from both GLEAM and GLDAS was resampled to a spatial resolution of 0.5°.

2.1.2. Satellite Measurements of Forest Canopy

To reconstruct the short-term canopy dieback related to forest mortality, we used satellite measurements of both the normalized difference vegetation index (NDVI) and VOD. NDVI is an optical indicator for describing forest canopy greenness and has been widely used in forest mortality monitoring at the regional scale (Hart & Veblen, 2015; Rogers et al., 2018). Biweekly NDVI time series were acquired from the Global Inventory Modeling and Mapping Studies (GIMMS) NDVI3g data set with a spatial resolution of 0.0833° (https://climate-dataguide.ucar.edu/climate-data/ndvi-normalized-difference-vegetation-index-3rd-generation-nasagfsc-gimms). The GIMMS NDVI3g data set was derived from the National Oceanic and Atmospheric Administration

23284277, 2024, 1, Downloaded from https://agupubs.onlinelibrary.wiley.com/doi/10.1029/2023EF003705 by Cochrane France, Wiley Online Library on [11/01/2024]. See the Terms and Conditions (https://onlinelibrary.wiley.com/terms-and-conditions) on Wiley Online Library for rules of use; OA articles are governed by the applicable Creative Commons License

10.1029/2023EF003705

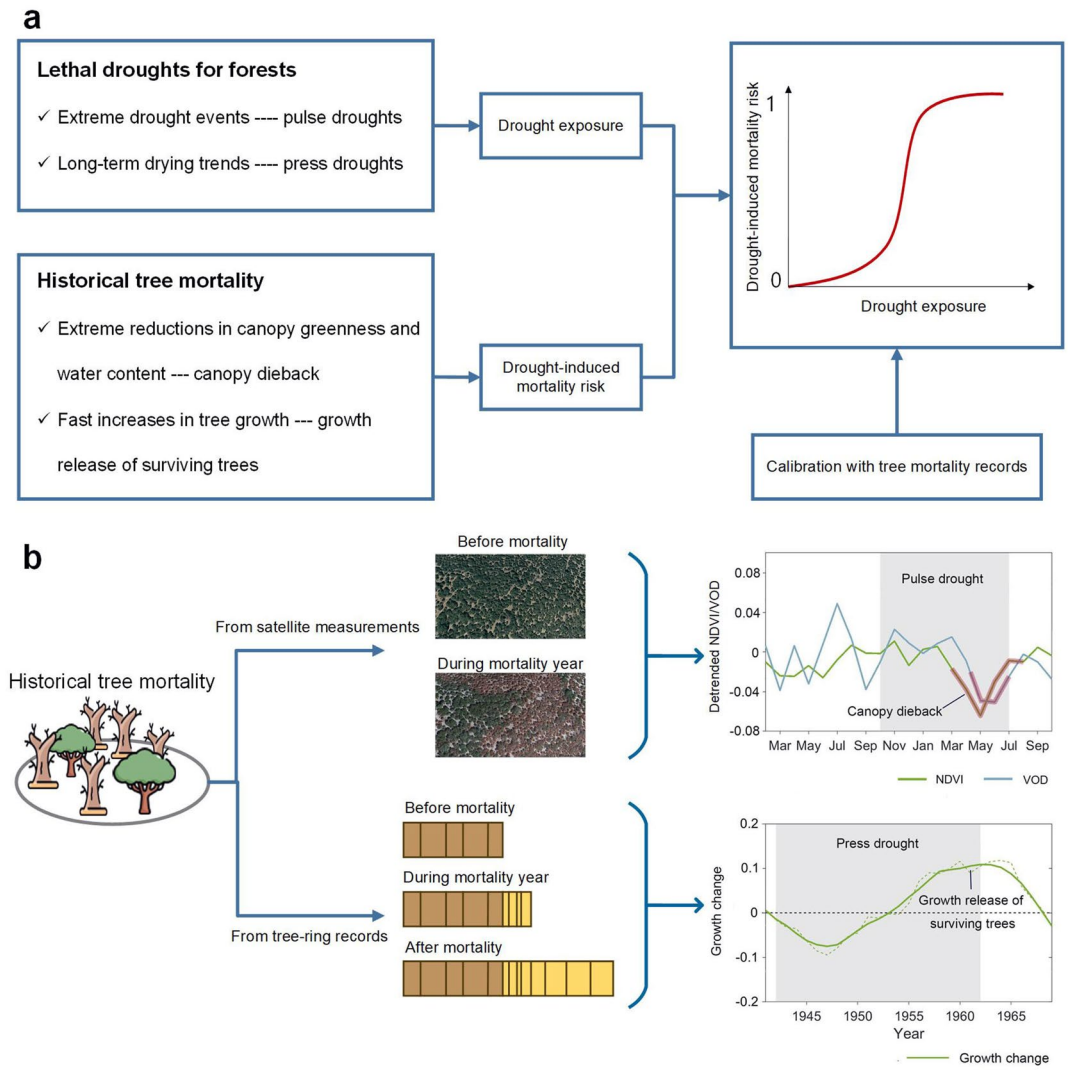

Figure 1. Method framework of this study. (a) Roadmap of relationship between forest mortality risk and two types of droughts. (b) Potential mortality events derived from satellite measurement-based canopy dieback during mortality and tree-ring record-based growth release of surviving trees after mortality.

(NOAA)/Advanced Very High Resolution Radiometer (AVHRR) satellites (Pinzon & Tucker, 2014) and covers the period from 1982 to 2015. The larger 15-day NDVI was adopted for each month to produce monthly NDVI time series.

Although satellite measurements of NDVI contribute to capturing reduced canopy greenness, water content is also an indispensable indicator reflecting canopy dieback and drought-induced mortality (Martinez-Vilalta et al., 2019). The VOD time series describes the attenuation of radiation by vegetation, which is an ideal indicator of vegetation water content. Recently, VOD has been used in applications for forest mortality monitoring at a large scale (Rao et al., 2019; Verbesselt et al., 2016). Daily VOD time series were obtained from the VOD Climate Archive with a spatial resolution of 0.25° (https://zenodo.org/record/2575599) (Moesinger et al., 2019). The VOD time series were merged from various spaceborne sensors (Moesinger et al., 2019). Here, we used the Vegetation Optical Depth Climate Archive (VODCA) product for the Ku-band, which contains the longest time span (1987–2017). We averaged the daily VOD time series to monthly data.

Both satellite data sets were aggregated to a spatial resolution of 0.5° to match the drought indices. We used the overlapping time span (1988–2015) for the NDVI and VOD data sets.

23284277, 2024, 1, Downloaded from https://agupubs.onlinelibrary.wiley.com/doi/10.1029/2023EF003705 by Cochrane France, Wiley Online Library on [11/01/2024]. See the Terms and Conditions (https://onlinelibrary.wiley.com/terms-and-conditions) on Wiley Online Library for rules of use; OA articles are governed by the applicable Creative Commons License

23284277, 2024, 1, Downloaded from https://agupubs.onlinelibrary.wiley.com/doi/10.1029/2023EF003705 by Cochrane France, Wiley Online Library on [11/01/2024]. See the Terms and Conditions (https://onlinelibrary.wiley.com/terms-and-conditions) on Wiley Online Library for rules of use; OA articles are governed by the applicable Creative Commons License

2.1.3. Tree-Ring Width Records

To reconstruct the long-term canopy dieback related to forest mortality, we used tree ring width indices were obtained from the International Tree-Ring Data Bank (Grissino-Mayer & Fritts, 1997) (ITRDB, https://www.ncdc.noaa.gov/data-access/paleoclimatology-data/datasets/tree-ring). This database is the largest open-access tree ring database in the world and includes tree ring width data and detrended and standardized mean series of ring-width indices or chronologies. To better quantify growth change dynamics at the site level, we chose to use raw series of ring-width indices to estimate the disturbance history of forests. All available tree ring indices that satisfied the following four conditions were chosen: (a) at least five tree core samples collected in each site; (b) at least 50% of samples covered more than 50 years during the period from 1901 to 2017; (c) each ring width index derived from a measurement of tree ring width without splicing or deleting; and (d) locations and tree species recorded. In summary, we obtained data from 119,588 cores sampled at 3,218 sites, corresponding to 196 tree species belonging to 48 genera, of which 23 genera were angiosperms and 25 genera were gymnosperms.

2.1.4. CO_2 Concentration

We used global average atmospheric CO_2 concentration reported by the US National Oceanic and Atmospheric Administration Earth System Research Laboratory (NOAA/ESRL) (Lan et al., 2023), for the period between 1980 and 2010. The annual global CO_2 concentration is constructed by averaging half-hourly latitudinal CO_2 concentrations interpolated from the measurements of all NOAA/ESRL sites (Masarie & Tans, 1995).

2.1.5. Tree Mortality Database

We calibrated our model using the drought-induced tree mortality database that was collected from the literature (Hammond et al., 2022) and made available at the website of the International Tree Mortality Network at https://tree-mortality.net. This database contains locations, tree species most impacted, and the year of tree mortality events caused by dry and/or hot spells. In this study, we used the locations of 1,303 ground-based plots where tree mortality events were documented, including detailed locations and observed years of mortality.

2.1.6. Forest Definition

According to the Food and Agriculture Organization of the United Nations (FAO), forest is defined as "land spanning more than 0.5 ha with trees higher than 5 m and a canopy cover of more than 10%" (FAO, 2020). Considering that the spatial resolution of 0.5° in this study may result in mixed information from different vegetation types, we increased the canopy cover threshold to 20%. Using the global tree cover data at a resolution of 30 m (Hansen et al., 2013), we extracted forest-dominant grid cells that meet the following criteria: (a) tree cover >20%. (b) a $0.5° \times 0.5°$ cell covering more than 50% of the 30-m cell with tree cover >20%.

2.2. Relationship Between Drought Exposure and DMR

2.2.1. Definition and Quantification of Pulse Droughts

Pulse droughts are defined as periods when drought indices (PDSI and SPEI) were below the 95th quantile of the distribution of each grid cell. Both PDSI- and SPEI-derived pulse droughts were extracted from 1901 to 2017. Metrics describing the effects of pulse droughts are usually based on single event characteristics, for example, drought intensity, which may underestimate the impacts of extended drought periods on trees. Therefore, we used DE as a metric describing the impacts of pulse droughts, and calculated it as the integral of the drought index anomaly during each pulse drought, as Equation 1:

$$\mathrm{DE} = \left| \int_{a}^{b} f(x-\mu)dx \right| \tag{1}$$

where x and μ are the drought index and its multiyear average, respectively, and a and b are the start and end of each pulse drought, respectively. The absolute value of the integral was used to exclude the influence of the drought index's sign on the DE estimation.

2.2.2. Definition and Quantification of Press Droughts

A press drought is regarded as a long-term period with enhanced DE. We evaluated the drought change by calculating the difference between the preceding and subsequent 10-year DE means. Press droughts are defined as

23284277, 2024, 1, Downloaded from https://agupubs.onlinelibrary.wiley.com/doi/10.1029/2023EF003705 by Cochrane France, Wiley Online Library on [11/01/2024]. See the Terms and Conditions (https://onlinelibrary.wiley.com/terms-and-conditions) on Wiley Online Library for rules of use; OA articles are governed by the applicable Creative Commons License

periods when the differences are greater than zero, during which DE shows an increasing trend. The occurrence of a press drought is resulted from either an escalation in the magnitude and duration of pulse droughts or an elevation in their frequency. Consequently, in the definition of press drought, we take into account both the time lag effect of individual pulse droughts and the cumulative time lag effect caused by repeated pulse droughts. To quantify the effects of press droughts, we calculated the maximum magnitude of enhanced DE as Equation 2:

$$\Delta DE = \max_{[c,d]}(DE_s - DE_p) \tag{2}$$

where c and d are the start and end of each press drought, respectively. DE_p and DE_s are the preceding and subsequent 10-year DE means.

2.2.3. Drought-Induced Mortality Risk

We used satellite measurements of vegetation greenness and water content and a growth change index derived from tree ring records to measure canopy dieback or disturbance, which were treated as a proxy for historical forest mortality.

For pulse droughts, given that satellite-based forest canopy mortality has been mapped at a spatial grain of 0.5° in Europe (Senf et al., 2020), we identified forest mortality, at the same spatial resolution, as periods with extreme reductions in both canopy greenness (NDVI) (Pinzon & Tucker, 2014) and water content (VOD) (Moesinger et al., 2019) following pulse droughts (Figure 1b). Extreme reduction here is defined as NDVI and VOD decreasing below a certain percentile of the 1988–2015 distribution of each grid cell. In different climatic zones, we calibrated the percentiles of reduction of these indices using known mortality events (Hammond et al., 2022). The percentile that captures 70% of tree mortality events is regarded as the threshold in the corresponding climatic zone (Figure S1 and Table S1 in Supporting Information S1). Before identifying extreme reductions, we applied singular spectrum analysis to exclude the seasonal components of the NDVI and VOD time series. Considering the widespread greening trends of vegetation (Chen et al., 2019; Keenan & Riley, 2018; Zhu et al., 2016), we further detrended the NDVI time series by linear regression. The growing season here was roughly defined as April to October for the extratropical Northern Hemisphere (23°–90°N), previous-year October to current-year April for the extratropical Southern Hemisphere (23°–90°S), and the whole year for the tropical region (23°S–23°N) (Jiang et al., 2019). From 1988 to 2015, a period that both growing-season NDVI and growing-season VOD concurrently decreased during a pulse drought, and lasted for longer than six weeks was eventually recognized as a forest mortality event. To avoid a possible replicated calculation between the drought-induced mortality risk index (DMR) of pulse and press droughts, we considered only the canopy dieback that occurred during a pulse drought, without considering the lagged effects of droughts. The DMR of pulse droughts was estimated as the probability of satellite NDVI and VOD falling below thresholds during growing season droughts.

In the long run (e.g., 10–20 years), forest mortality is usually associated with a drought-induced growth decline of surviving individual trees (Williams et al., 2013) and their subsequent growth recovery because of reduced tree-to-tree competition (Splechtna et al., 2005; Wu et al., 2014). Therefore, we assumed that forest mortality in press drought coincides with growth decline and subsequent growth release, which can be identified based on the deficits and overshoots in radial growth changes. The DMR of press droughts was estimated as the probability of tree ring-derived deficits and subsequent overshoots coinciding with press droughts. Radial growth change was calculated using Equation 3 (Nowacki & Abrams, 1997):

$$\%GC = \frac{M_2 - M_1}{M_1} \times 100 \tag{3}$$

where %GC represents the percent growth change between the preceding and subsequent 10-year means and M_1 and M_2 are the preceding and subsequent 10-year ring-width means, respectively. We tested the effect of different moving windows on the relationship between radial growth change and drought indices. The correlation relationship between radial growth change and climate decreased from 0.18 to 0.07 with increasing length of the moving window (Figure S2 in Supporting Information S1), indicating that a longer temporal window could average out the short-term growth responses due to favorable climatic conditions (Jiang et al., 2019) and thus made the growth change index better capture the growth increases commonly associated with canopy disturbance (Nowacki & Abrams, 1997). In the end, we used the 10-year span for the mean of ring-widths, which is widely used to identify canopy disturbance (Nowacki & Abrams, 1997; Splechtna et al., 2005; Wu et al., 2014). A master

23284277, 2024, 1, Downloaded from https://agupubs.onlinelibrary.wiley.com/doi/10.1029/2023EF003705 by Cochrane France, Wiley Online Library on [11/01/2024]. See the Terms and Conditions (https://onlinelibrary.wiley.com/terms-and-conditions) on Wiley Online Library for rules of use; OA articles are governed by the applicable Creative Commons License

growth-change series for each site was built by averaging the %GC for all trees in each site. A site-averaged %GC < 0 was identified as growth decline, and a %GC > 0 was identified as growth release after canopy dieback or the death of affected trees. An overshoot in %GC was assumed to occur within 10 years after a press drought, which is the maximum time lag between a press drought and growth release at the global scale (Figure S3 in Supporting Information S1). In addition, an overshoot in %GC without a previous water deficit was recognized as a growth release possibly caused by logging, fire or very favorable climate (e.g., wet conditions) and was excluded from subsequent calculations.

The DMR was defined as the probability of mortality events, given the occurrence of pulse and/or press droughts in each grid cell and for each location with available tree-ring data as Equation 4:

$$\mathrm{DMR} = \frac{D_m}{D_t} \times w \tag{4}$$

where D_m is the number of pulse/press droughts coinciding with forest mortality and D_t is the total number of historical pulse/press droughts in each grid cell or tree ring site. To avoid overestimation due to the number of historical droughts being the denominator, we multiplied the fraction by a weight w, which was calculated as the quotient between the number of historical droughts in each grid cell or site and the average number of historical droughts in each climatic zone. Note that the spatial resolution of our mortality detection using satellite data does not allow for the identification of climate change-induced diffuse forest mortality, that is, the death of few individual trees dispersed within an otherwise intact forest cover (Hartmann et al., 2018). Therefore, DMR here indicates forest mortality risk at regional scale, contrasting from the binary response (dead or alive) of tree mortality at the individual level (Martinez-Vilalta et al., 2019).

2.2.4. DMR Estimates

Based on the relationship between DMR and DE/ΔDE for pulse and press droughts, DMR can be predicted using Equation 5:

$$\mathrm{DMR} = \begin{cases} a_1 \cdot e^{-a_2 \cdot \mathrm{DE}} + a_0, & \text{pulse drought} \\ b_1 \cdot e^{-b_2 \cdot \Delta\mathrm{DE}} + b_0, & \text{press drought} \end{cases} \tag{5}$$

where DMR is the overall drought-induced mortality risk, DE is the DE during pulse droughts, and ΔDE is the maximum magnitude of enhanced DE during press droughts (all coefficients are shown in Tables S2 in Supporting Information S1). For different climatic zones, we used different coefficients to estimate DMR. Considering that the compounded stress from both extreme droughts and long-term dry trends have been observed to exacerbate tree mortality (Barbeta et al., 2015; Matusick et al., 2018), forest mortality risk is calculated as the sum of pulse and press drought if they occurred synchronously.

2.2.5. Estimation Accuracy

The DMR values in 1,303 mortality locations were extracted and compared with global DMR over the same period (1988–2010). A total of 91.4% of tree mortality events were captured by the DMR index (DMR > 0), suggesting a high accuracy of DMR estimates. Considering the potential false positives, however, a reliable threshold is needed to identify forest mortality. Since a record of all true mortality events at the global scale is absent, we examined the false positive rate in 1,303 locations of tree mortality records (Hammond et al., 2022). We plotted the receiver operating characteristic (ROC) curve for DMR in 1,303 locations from 1980 to 2010 and calculated the areas under the ROC curve (AUC). The optimal threshold was identified according to Equation 6 (Unal, 2017):

$$\min\{|\mathrm{TPR} - \mathrm{AUC}| + |1 - \mathrm{FPR} - \mathrm{AUC}|\} \tag{6}$$

where TPR is the true positive rate and FPR is the false positive rate. AUC across mortality locations is 0.80, which is considered acceptable (Mandrekar, 2010). A threshold that minimizes this function and the difference between true and false positive rates will be labeled a high mortality risk threshold that best differentiates with and without elevated forest mortality.

10.1029/2023EF003705

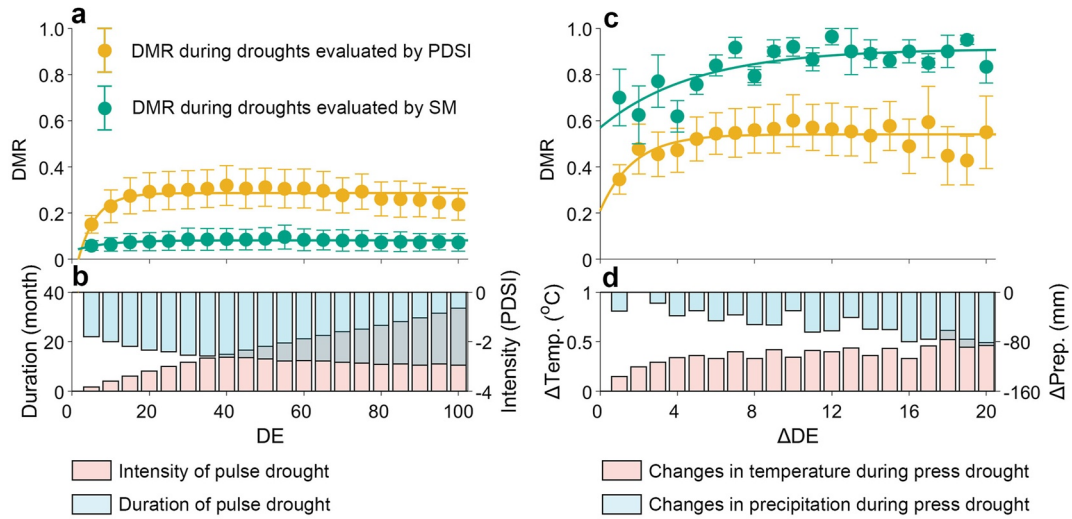

Figure 2. Relationship between drought-induced mortality risk (drought-induced mortality risk index (DMR)) and drought exposure (DE). (a) Response of DMR to DE during pulse droughts. (b) Changes in drought intensity (red bars) and duration (blue bars) with DE. (c) Response of DMR to enhanced DE (ΔDE) during press droughts. (d) Changes in temperature (ΔTemp., red bars) and precipitation (ΔPrep., blue bars) with enhanced DE (ΔDE). Two drought indices were used to estimate DE and ΔDE in this figure: Palmer Drought Severity Index and soil moisture from Global Land Evaporation Amsterdam Model (SM).

3. Results

The DMR of pulse droughts (derived from PDSI and SPEI) increases from 0 to 0.28 with synchronous increases of both drought intensity and duration (adjusted R^2 between DMR and DE is 0.61, Figure 2a and Figure S4a in Supporting Information S1). However, DMR saturates with increases in drought duration (droughts lasting over 8 months), as long as drought intensity remains the same (Figure 2b). However, DMR has an insignificant relationship with the exposure of pulse droughts (derived from soil moisture), indicating that rising CO_2 may alleviate the effects of pulse droughts on mortality risk (Figure 2a and Figure S4c in Supporting Information S1).

During press droughts, an increase in ΔDE enhanced DMR from 0.27 to 0.57 (PDSI-derived press droughts) and from 0.59 to 0.85 (soil moisture-derived press droughts, Figure 2c). We further tested the relationship between DMR and changes in temperature and precipitation, as press droughts can be driven by long-term reductions in precipitation and/or increased evapotranspiration due to temperature rising. DMR is significantly correlated with changes of temperature during press droughts ($R = 0.49$, $P < 0.05$), but not with changes in precipitation ($R = -0.36$, $P = 0.12$, Figure 2d), suggesting the crucial role of hotter droughts on increases of forest mortality risk. Interestingly, we observed increases in DMR with press droughts derived from both PDSI and GLEAM-soil moisture (Figure 2c). Furthermore, DMR responded more strongly to long-term DE derived from soil moisture, suggesting that rising CO_2 fails to reduce mortality risk on a long-term scale and may even increase it in turn. Stronger response of DMR was also observed to press droughts derived from GLDAS-soil moisture, compared to that derived from SPEI (Figures S4b and S4d in Supporting Information S1).

Taking into account the uneven sampling in ITRDB data and the preference for specific tree species depending on the sampling objectives may lead to a potential for bias in the results, we conducted a more focused analysis by segregating the tree-ring data into two categories: gymnosperms and angiosperms. Reassuringly, our analysis did not reveal any significant differences in the response of DMR to DE between gymnosperms and angiosperms (Figures S5a–S5b in Supporting Information S1). Furthermore, we isolated individual genus that had available data from more than 50 sites for separate analysis. A notable increase in DMR with increasing DE was observed within each of the analyzed genus (Figures S5c–S5h in Supporting Information S1).

Responses of DMR to both pulse and press droughts are robust when applied in different climatic zones (0.33 < adjusted R^2 < 0.91, Figures S6 and S7 in Supporting Information S1). Based on the relationship between DMR and DE/ΔDE for pulse and press droughts, we calculated the total DMR due to both pulse and press droughts in the past 100 years and compared our historical DMR estimates with 1,303 published ground-based

23284277, 2024, 1, Downloaded from https://agupubs.onlinelibrary.wiley.com/doi/10.1029/2023EF003705 by Cochrane France, Wiley Online Library on [11/01/2024]. See the Terms and Conditions (https://onlinelibrary.wiley.com/terms-and-conditions) on Wiley Online Library for rules of use; OA articles are governed by the applicable Creative Commons License

10.1029/2023EF003705

23284277, 2024, 1, Downloaded from https://agupubs.onlinelibrary.wiley.com/doi/10.1029/2023EF003705 by Cochrane France, Wiley Online Library on [11/01/2024]. See the Terms and Conditions (https://onlinelibrary.wiley.com/terms-and-conditions) on Wiley Online Library for rules of use; OA articles are governed by the applicable Creative Commons License

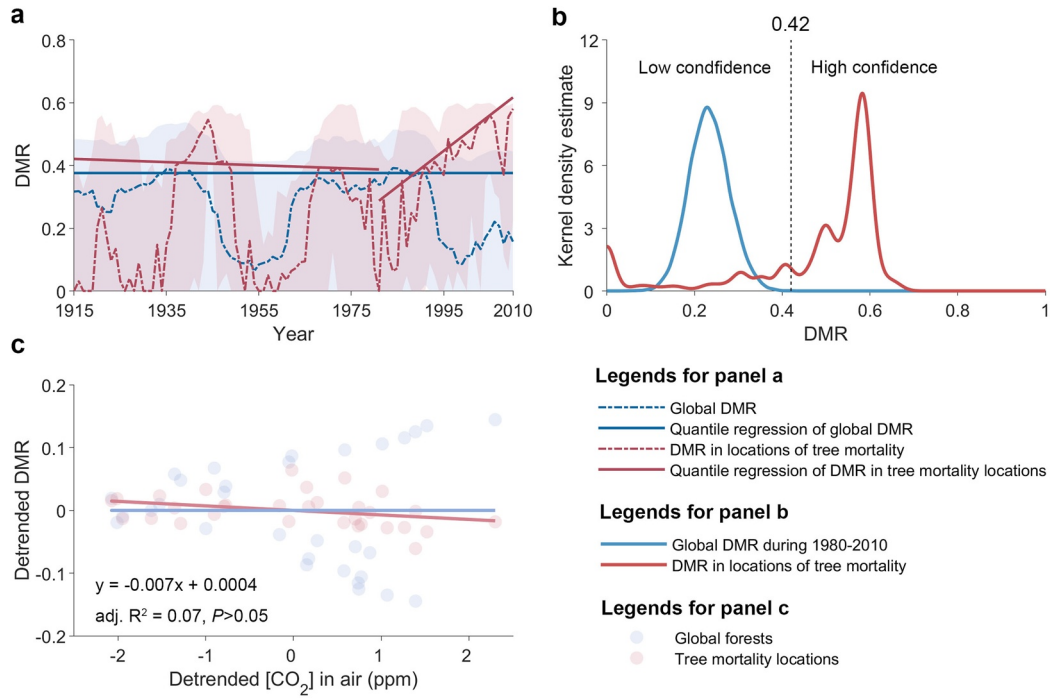

Figure 3. Estimation of drought-induced mortality risk (drought-induced mortality risk index (DMR)) and exclusion of CO_2 fertilization effect. (a) Annual changes in DMR at the global scale (blue lines) and across 1,303 locations of tree mortality events (red lines) during 1915–2010. (b) Probability density function of the global DMR from 1988 to 2010 (blue line) and in locations of tree mortality events (red line). The vertical dashed line indicates the optimal threshold for identifying tree mortality (0.42). (c) Relationship between detrended CO_2 concentration [CO_2] in air and detrended DMR across global forests (blue points) and locations with tree mortality records (red points).

observations of tree mortality. From 1915 to 2010, the global estimated DMR varied with a maximum value of 0.37 at different periods (Figure 3a). However, DMR across mortality locations has significantly increased since 1980 (Mann-Kendall test, $p < 0.05$, Figure 3a) and greatly exceeded global DMR over the same period (median value: 0.50 vs. 0.23). In total, 91.4% of the tree mortality events had DMR over zero during the mortality year (Figure 3b). But considering potential false positives due to the loose threshold, we plotted ROC curve for DMR in these mortality locations from 1980 to 2010. The DMR on the optimal threshold of ROC is 0.42, corresponding to a false positive rate of 0.33 and a true positive rate of 0.80 (Figure S8 in Supporting Information S1). We identified DMR = 0.42 as a threshold that could best differentiate between sites with and without elevated forest mortality. DMR across mortality locations exceeded the threshold of 0.42 since 1996. From 1980 to 2010, changes in atmospheric CO_2 concentration were insignificantly but negatively related to DMR across mortality locations (Figure 3c), indicating a slight alleviating effect of increasing CO_2 concentration on the total mortality risk but not actually preventing the increase of tree mortality.

The DMR estimates allow drawing geographic patterns of potential global forest loss due to enhanced drought stress. DMR across global forested areas was relatively low before the industrial (1930–1960), with DMR in only 1.9% of the areas exceeding the threshold of 0.42 (Figure 4a). However, this fraction increased to 7.4% during 1980–2010 (Figure 4b), indicating that approximately 0.28 billion hectares of forested areas were threatened by droughts, especially the long-term stress of press droughts. Although areas with high mortality risk were sparsely distributed globally, for example, in Mediterranean areas, south Africa and far east Siberia, it did be much more than observed records.

4. Discussion

We observed increasing mortality risk with exposure to both pulse and press droughts, which allows for quantifying lethal drought stress on global forests and identifying the hotspots of forest mortality. Hydraulic failure could explain the increased risk of forest mortality during pulse droughts. Because of hydraulic dysfunction, trees may

10.1029/2023EF003705

23284277, 2024, 1, Downloaded from https://agupubs.onlinelibrary.wiley.com/doi/10.1029/2023EF003705 by Cochrane France, Wiley Online Library on [11/01/2024]. See the Terms and Conditions (https://onlinelibrary.wiley.com/terms-and-conditions) on Wiley Online Library for rules of use; OA articles are governed by the applicable Creative Commons License

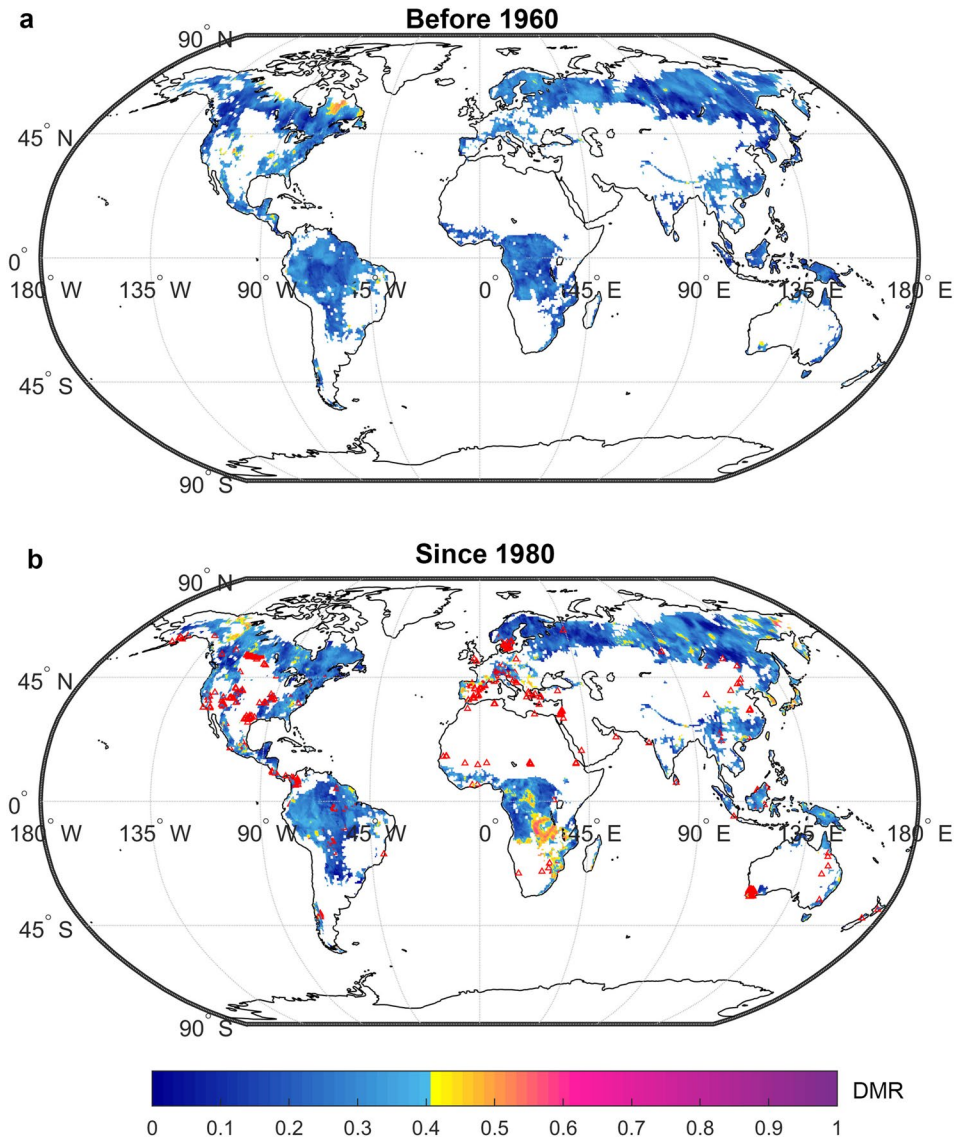

Figure 4. Patterns of estimated drought-induced mortality risk index (DMR) in global forests. 30-year average of DMR during (a) 1930–1960, (b) 1980–2010. Red triangles in panel (a) indicates documented tree mortality sites in the literature.

experience 3–6 months of cessation of stem sap flow, pass lethal thresholds in hydraulic failure and eventually die (Hammond et al., 2019; Preisler et al., 2021). But during an extended pulse drought, for example, droughts lasting over 8 months in our study, more drought-tolerant tree species or individuals could survive through structural and functional acclimation to drought, for example, leaf shedding, xylem regrowth (Gauthey et al., 2022) or shifts to a more conservative water-use strategy (Cinnirella et al., 2002), thus preventing further increases of mortality risk. Including plant responses to CO_2 reduced the mortality risk of pulse droughts, because the high concentration of CO_2 allows plants to reduce stomatal conductance without negative feedback on photosynthetic rates during non-drought periods, which increases the water use efficiency of plants and reduces the risk of carbon starvation (Ainsworth & Rogers, 2007).

Different from hydraulic failure in pulse droughts, while not leading to rapid mortality of trees, press droughts could gradually hamper tree physiological processes and cause slow changes in forests, for example, by weakening the recovering ability of trees through lowering carbon uptake and transport (Berdanier & Clark, 2016; McDowell et al., 2008) or by changing background mortality rates of forests over decades due to increased physiological stress and vulnerability against biotic stressors (Van Mantgem et al., 2009). In our framework, including

23284277, 2024, 1, Downloaded from https://agupubs.onlinelibrary.wiley.com/doi/10.1029/2023EF003705 by Cochrane France, Wiley Online Library on [11/01/2024]. See the Terms and Conditions (https://onlinelibrary.wiley.com/terms-and-conditions) on Wiley Online Library for rules of use; OA articles are governed by the applicable Creative Commons License

CO_2 effects leads to relatively higher mortality risk in press droughts, indicating a negligible and even potentially negative effect of CO_2 concentration on mortality risk. Enhanced water use efficiency by rising CO_2 can stimulate growth but may also lead to structural overshoot (Jump et al., 2017), with greater stand-level competition for resources such as nutrients and water (Zhang et al., 2021), which may predispose trees to greater mortality under subsequent pulse drought (Hartmann et al., 2022; McDowell et al., 2018). At present, precise quantification of the CO_2 effects on soil moisture over past decades remains elusive. Nevertheless, employing the GLEAM and GLDAS products, which closely approximate actual soil moisture values, stands out as the most efficient method for investigating CO_2 effects within empirical studies of forest mortality risk. This is because any potential reduction in transpiration caused by the rising CO_2 levels (if it indeed exists) may already be encompassed in the dynamic changes of soil moisture. Recent studies involving modeled $CO_2 \times$ drought experiments further corroborate our findings, demonstrating that in conditions of prolonged water stress, the capacity of increased plant water-use efficiency to alleviate drought stress was negligible (De Kauwe et al., 2021, 2022).

Our results suggested that the sustainability of global forests is challenged by increasing drought stress, although restoring forested biomes is needed to partially offset anthropogenic CO_2 emissions. In the past 30 years, both restoration and afforestation led to increased global forest cover that counterbalanced some of the regional forest loss due to drought-induced tree mortality (Song et al., 2018). However, drought threats to forests were observed to increase across 0.28 billion hectares of forested areas since the 1980s, especially the compounded exposure of both pulse and press droughts. Existing and potential new forests might be more susceptible to drought-induced mortality (Hartmann et al., 2022), as global terrestrial environments are projected toward a substantial drying trend at the end of this century (Naumann et al., 2018; Scheff & Frierson, 2015; Trenberth et al., 2014). Despite CO_2 fertilization can alleviate short-term drought stress (Swann et al., 2016; Yang et al., 2019) and efficiently reduce forest mortality risk in high warming scenarios (Liu et al., 2017), our results suggested the capacity of rising CO_2 to ameliorate long-term drought stress and reduce mortality risk is limited, as press drought is increasing due to anthropogenic warming (Chiang et al., 2021), for example, the ongoing North American megadrought (Williams et al., 2020) and the associated increase of forest mortality (Hember et al., 2017; McNellis et al., 2021; Van Mantgem et al., 2009).

Drought exposure and ecological risk assessments under climate change are the basis for effective management of climate risks (Field et al., 2012). Our empirical estimations indicate a high risk of forest cover loss and corroborate modeling approaches that also estimate carbon loss in forest ecosystems due to climate change (Scholze et al., 2006; Sitch et al., 2008). Ensuing losses may be substantial as background mortality rates increase (Hartmann et al., 2018), and as unprecedented hotter-drought extreme events increase non-linearly (Alizadeh et al., 2020). Note that this approach in our study may underestimate the true risk as satellite measurements may not always capture all events reliably, even strong mortality events (Hartmann et al., 2022).

5. Conclusions

We observed that forest mortality risk increases with DE, and rising CO_2 can only alleviate drought stress at a short-term scale. In the past few decades, forested areas far more than we have observed have been fatally threatened by drought. Our study provides an empirical framework for a better prediction of tree mortality. We therefore suggest data assimilation from different proxies of tree mortality, including satellite measurements, tree-ring records, long-term forest inventories and so on, to improve the monitoring of forest mortality globally, and also pay more attention to forest mortality driven by press droughts.

Conflict of Interest

The authors declare that they have no competing interests.

Data Availability Statement

The estimates of DE for pulse and press droughts and DMR are available in Xu (2023). All data needed to evaluate the conclusions are open accessed. The PDSI was obtained from the Climatic Research Unit at the University of East Anglia (Osborn et al., 2018). Standardized Precipitation-Evapotranspiration Index was obtained from Global SPEI database (Vicente-Serrano et al., 2010). Soil moisture were obtained from GLEAM (Martens

et al., 2017) and GLDAS (Rodell et al., 2004). Global Inventory Modeling and Mapping Studies NDVI was from the NOAA/AVHRR satellites (Pinzon & Tucker, 2014). Vegetation optical depth was obtained from the VOD Climate Archive (Moesinger et al., 2019). Tree ring width indices were obtained from the International Tree-Ring Data Bank (Grissino-Mayer & Fritts, 1997). Tree mortality database (Hammond et al., 2022) is in the International Tree Mortality Network's Global Tree Mortality Database. Requests for further information and resources should be directed to the corresponding author.

Acknowledgments
This work was granted by National Key Research and Development Program of China (2022YFF0801803) and National Natural Science Foundation of China (41901057, 42161144008).

References

Adams, H. D., Zeppel, M. J. B., Anderegg, W. R. L., Hartmann, H., Landhäusser, S. M., Tissue, D. T., et al. (2017). A multi-species synthesis of physiological mechanisms in drought-induced tree mortality. *Nature Ecology & Evolution*, *1*(9), 1285–1291. https://doi.org/10.1038/s41559-017-0248-x

Ainsworth, E. A., & Rogers, A. (2007). The response of photosynthesis and stomatal conductance to rising [CO_2]: Mechanisms and environmental interactions. *Plant, Cell and Environment*, *30*(3), 258–270. https://doi.org/10.1111/j.1365-3040.2007.01641.x

Alizadeh, M. R., Adamowski, J., Nikoo, M. R., AghaKouchak, A., Dennison, P., & Sadegh, M. (2020). A century of observations reveals increasing likelihood of continental-scale compound dry-hot extremes. *Science Advances*, *6*(39), eaaz4571. https://doi.org/10.1126/sciadv.aaz4571

Allen, C. D., Breshears, D. D., & Mcdowell, N. G. (2015). On underestimation of global vulnerability to tree mortality and forest die-off from hotter drought in the Anthropocene. *Ecosphere*, *6*(8), 1–55. https://doi.org/10.1890/ES15-00203.1

Anderegg, W. R. L., Trugman, A. T., Badgley, G., Konings, A. G., & Shaw, J. (2020). Divergent forest sensitivity to repeated extreme droughts. *Nature Climate Change*, *10*(12), 1091–1095. https://doi.org/10.1038/s41558-020-00919-1

Ault, T. R. (2020). On the essentials of drought in a changing climate. *Science*, *368*(6488), 256–260. https://doi.org/10.1126/science.aaz5492

Barbeta, A., Mejía-Chang, M., Ogaya, R., Voltas, J., Dawson, T. E., & Peñuelas, J. (2015). The combined effects of a long-term experimental drought and an extreme drought on the use of plant-water sources in a Mediterranean forest. *Global Change Biology*, *21*(3), 1213–1225. https://doi.org/10.1111/gcb.12785

Bauman, D., Fortunel, C., Delhaye, G., Malhi, Y., Cernusak, L. A., Bentley, L. P., et al. (2022). Tropical tree mortality has increased with rising atmospheric water stress. *Nature*, *608*(7923), 528–533. https://doi.org/10.1038/s41586-022-04737-7

Berdanier, A. B., & Clark, J. S. (2016). Multiyear drought-induced morbidity preceding tree death in southeastern U.S. forests. *Ecological Applications*, *26*(1), 17–23. https://doi.org/10.1890/15-0274

Bonan, G. B. (2008). Forests and climate change: Forcings, feedbacks, and the climate benefits of forests. *Science*, *320*(5882), 1444–1449. https://doi.org/10.1126/science.1155121

Brodribb, T. J., Powers, J., Cochard, H., & Choat, B. (2020). Hanging by a thread? Forests and drought. *Science*, *368*(6488), 261–266. https://doi.org/10.1126/science.aat7631

Chen, C., Park, T., Wang, X., Piao, S., Xu, B., Chaturvedi, R. K., et al. (2019). China and India lead in greening of the world through land-use management. *Nature Sustainability*, *2*(2), 122–129. https://doi.org/10.1038/s41893-019-0220-7

Chiang, F., Mazdiyasni, O., & AghaKouchak, A. (2021). Evidence of anthropogenic impacts on global drought frequency, duration, and intensity. *Nature Communications*, *12*(1), 2754. https://doi.org/10.1038/s41467-021-22314-w

Cinnirella, S., Magnani, F., Saracino, A., & Borghetti, M. (2002). Response of a mature Pinus laricio plantation to a three-year restriction of water supply: Structural and functional acclimation to drought. *Tree Physiology*, *22*(1), 21–30. https://doi.org/10.1093/treephys/22.1.21

Dai, A. (2011). Characteristics and trends in various forms of the Palmer Drought Severity Index during 1900–2008. *Journal of Geophysical Research*, *116*(D12), D12115. https://doi.org/10.1029/2010JD015541

De Kauwe, M. G., Medlyn, B. E., & Tissue, D. T. (2021). To what extent can rising [CO_2] ameliorate plant drought stress? *New Phytologist*, *231*(6), 2118–2124. https://doi.org/10.1111/nph.17540

De Kauwe, M. G., Sabot, M. E. B., Medlyn, B. E., Pitman, A. J., Meir, P., Cernusak, L. A., et al. (2022). Towards species-level forecasts of drought-induced tree mortality risk. *New Phytologist*, *235*(1), 94–110. https://doi.org/10.1111/nph.18129

FAO. (2020). Global forest resources assessment 2020: Main report. https://doi.org/10.4060/ca9825en

Field, C. B., Barros, V., Stocker, T. F., Qin, D., Dokken, D. J., Ebi, K. L., et al. (2012). *Managing the risks of extreme events and disasters to advance climate change adaptation*. Cambridge University Press.

Fisher, R. A., Koven, C. D., Anderegg, W. R. L., Christoffersen, B. O., Dietze, M. C., Farrior, C. E., et al. (2018). Vegetation demographics in Earth System Models: A review of progress and priorities. *Global Change Biology*, *24*(1), 35–54. https://doi.org/10.1111/gcb.13910

Gauthey, A., Peters, J. M. R., Lòpez, R., Carins-Murphy, M. R., Rodriguez-Dominguez, C. M., Tissue, D. T., et al. (2022). Mechanisms of xylem hydraulic recovery after drought in Eucalyptus saligna. *Plant, Cell and Environment*, *45*(4), 1216–1228. https://doi.org/10.1111/pce.14265

Grissino-Mayer, H. D., & Fritts, H. C. (1997). The International Tree-Ring Data Bank: An enhanced global database serving the global scientific community [Dataset]. The Holocene, *7*(2), 235–238. https://doi.org/10.1177/095968369700700212

Hammond, W. M., Williams, A. P., Abatzoglou, J. T., Adams, H. D., Klein, T., López, R., et al. (2022). Global field observations of tree die-off reveal hotter-drought fingerprint for Earth's forests [Dataset]. Nature Communications, *13*(1), 1761. https://doi.org/10.1038/s41467-022-29289-2

Hammond, W. M., Yu, K., Wilson, L. A., Will, R. E., Anderegg, W. R. L., & Adams, H. D. (2019). Dead or dying? Quantifying the point of no return from hydraulic failure in drought-induced tree mortality. *New Phytologist*, *223*(4), 1834–1843. https://doi.org/10.1111/nph.15922

Hansen, M. C., Potapov, P. V., Moore, R., Hancher, M., Turubanova, S. A., Tyukavina, A., et al. (2013). High-resolution global maps of 21st-century forest cover change. *Science*, *342*(6160), 850–853. https://doi.org/10.1126/science.1244693

Harris, R. M. B., Beaumont, L. J., Vance, T. R., Tozer, C. R., Remenyi, T. A., Perkins-Kirkpatrick, S. E., et al. (2018). Biological responses to the press and pulse of climate trends and extreme events. *Nature Climate Change*, *8*(7), 579–587. https://doi.org/10.1038/s41558-018-0187-9

Hart, S. J., & Veblen, T. T. (2015). Detection of spruce beetle-induced tree mortality using high- and medium-resolution remotely sensed imagery. *Remote Sensing of Environment*, *168*, 134–145. https://doi.org/10.1016/j.rse.2015.06.015

Hartmann, H., Bastos, A., Das, A. J., Esquivel-Muelbert, A., Hammond, W. M., Martínez-Vilalta, J., et al. (2022). Climate change risks to global forest health: Emergence of unexpected events of elevated tree mortality worldwide. *Annual Review of Plant Biology*, *73*(1), 673–702. https://doi.org/10.1146/annurev-arplant-102820-012804

Hartmann, H., Moura, C. F., Anderegg, W. R. L., Ruehr, N. K., Salmon, Y., Allen, C. D., et al. (2018). Research frontiers for improving our understanding of drought-induced tree and forest mortality. *New Phytologist*, *218*(1), 15–28. https://doi.org/10.1111/nph.15048

23284277, 2024, 1, Downloaded from https://agupubs.onlinelibrary.wiley.com/doi/10.1029/2023EF003705 by Cochrane France, Wiley Online Library on [11/01/2024]. See the Terms and Conditions (https://onlinelibrary.wiley.com/terms-and-conditions) on Wiley Online Library for rules of use; OA articles are governed by the applicable Creative Commons License

Hember, R. A., Kurz, W. A., & Coops, N. C. (2017). Relationships between individual-tree mortality and water-balance variables indicate positive trends in water stress-induced tree mortality across North America. *Global Change Biology*, *23*(4), 1691–1710. https://doi.org/10.1111/gcb.13428

Jiang, P., Liu, H., Piao, S., Ciais, P., Wu, X., Yin, Y., & Wang, H. (2019). Enhanced growth after extreme wetness compensates for post-drought carbon loss in dry forests. *Nature Communications*, *10*(1), 195. https://doi.org/10.1038/s41467-018-08229-z

Jump, A. S., Ruiz-Benito, P., Greenwood, S., Allen, C. D., Kitzberger, T., Fensham, R., et al. (2017). Structural overshoot of tree growth with climate variability and the global spectrum of drought-induced forest dieback. *Global Change Biology*, *23*(9), 3742–3757. https://doi.org/10.1111/gcb.13636

Keenan, T. F., & Riley, W. J. (2018). Greening of the land surface in the world's cold regions consistent with recent warming. *Nature Climate Change*, *8*(9), 825–828. https://doi.org/10.1038/s41558-018-0258-y

Lan, X., Tans, P., & Thoning, K. W. (2023). Trends in globally-averaged CO_2 determined from NOAA Global Monitoring Laboratory measurements. Version 2023-06. https://doi.org/10.15138/9N0H-ZH07

Liu, Y., Parolari, A. J., Kumar, M., Huang, C.-W., Katul, G. G., & Porporato, A. (2017). Increasing atmospheric humidity and CO_2 concentration alleviate forest mortality risk. *Proceedings of the National Academy of Sciences*, *114*(37), 9918–9923. https://doi.org/10.1073/pnas.1704811114

Liu, Y., Wang, A., An, Y., Lian, P., Wu, D., Zhu, J., et al. (2018). Hydraulics play an important role in causing low growth rate and dieback of aging Pinus sylvestris var. mongolica trees in plantations of Northeast China. *Plant, Cell and Environment*, *41*(7), 1500–1511. https://doi.org/10.1111/pce.13160

Mandrekar, J. N. (2010). Receiver operating characteristic curve in diagnostic test assessment. *Journal of Thoracic Oncology*, *5*(9), 1315–1316. https://doi.org/10.1097/jto.0b013e3181ec173d

Martens, B., Miralles, D. G., Lievens, H., van der Schalie, R., de Jeu, R. A. M., Fernández-Prieto, D., et al. (2017). GLEAM v3: Satellite-based land evaporation and root-zone soil moisture [Dataset]. Geoscientific Model Development, *10*(5), 1903–1925. https://doi.org/10.5194/gmd-10-1903-2017

Martinez-Vilalta, J., Anderegg, W. R. L., Sapes, G., & Sala, A. (2019). Greater focus on water pools may improve our ability to understand and anticipate drought-induced mortality in plants. *New Phytologist*, *223*(1), 22–32. https://doi.org/10.1111/nph.15644

Masarie, K. A., & Tans, P. P. (1995). Extension and integration of atmospheric carbon dioxide data into a globally consistent measurement record. *Journal of Geophysical Research*, *100*(D6), 11593–11610. https://doi.org/10.1029/95jd00859

Matusick, G., Ruthrof, K. X., Kala, J., Brouwers, N. C., Breshears, D. D., & Hardy, G. E. S. J. (2018). Chronic historical drought legacy exacerbates tree mortality and crown dieback during acute heatwave-compounded drought. *Environmental Research Letters*, *13*(9), 095002. https://doi.org/10.1088/1748-9326/aad8cb

McDowell, N., Allen, C. D., Anderson-Teixeira, K., Brando, P., Brienen, R., Chambers, J., et al. (2018). Drivers and mechanisms of tree mortality in moist tropical forests. *New Phytologist*, *219*(3), 851–869. https://doi.org/10.1111/nph.15027

McDowell, N., Pockman, W. T., Allen, C. D., Breshears, D. D., Cobb, N., Kolb, T., et al. (2008). Mechanisms of plant survival and mortality during drought: Why do some plants survive while others succumb to drought? *New Phytologist*, *178*(4), 719–739. https://doi.org/10.1111/j.1469-8137.2008.02436.x

McNellis, B. E., Smith, A. M. S., Hudak, A. T., & Strand, E. K. (2021). Tree mortality in western U.S. forests forecasted using forest inventory and Random Forest classification. *Ecosphere*, *12*(3), e03419. https://esajournals.onlinelibrary.wiley.com/doi/abs/10.1002/ecs2.3419

Moesinger, L., Dorigo, W., De Jeu, R., Van der Schalie, R., Scanlon, T., Teubner, I., & Forkel, M. (2019). The Global long-term microwave vegetation optical depth climate archive VODCA (1.0) [Dataset]. Zenodo. https://doi.org/10.5281/zenodo.2575599

Naumann, G., Alfieri, L., Wyser, K., Mentaschi, L., Betts, R. A., Carrao, H., et al. (2018). Global changes in drought conditions under different levels of warming. *Geophysical Research Letters*, *45*(7), 3285–3296. https://doi.org/10.1002/2017gl076521

Nowacki, G. J., & Abrams, M. D. (1997). Radial-growth averaging criteria for reconstructing disturbance histories from presettlement-origin oaks. *Ecological Monographs*, *67*(2), 225–249. https://doi.org/10.1890/0012-9615(1997)067[0225:rgacfr]2.0.co;2

Osborn, T. J., Barichivich, J., Harris, I., van der Schrier, G., & Jones, P. (2018). Drought [in "state of the climate in 2017"]. [Dataset]. Bulletin of the American Meteorological Society, *99*, S36–S37. https://crudata.uea.ac.uk/cru/data/drought/

Pinzon, J. E., & Tucker, C. J. (2014). A non-stationary 1981–2012 AVHRR NDVI3g time series [Dataset]. Remote Sensing, *6*(8), 6929–6960. https://doi.org/10.3390/rs6086929

Preisler, Y., Tatarinov, F., Grünzweig, J. M., & Yakir, D. (2021). Seeking the "point of no return" in the sequence of events leading to mortality of mature trees. *Plant, Cell and Environment*, *44*(5), 1315–1328. https://doi.org/10.1111/pce.13942

Rao, K., Anderegg, W. R. L., Sala, A., Martínez-Vilalta, J., & Konings, A. G. (2019). Satellite-based vegetation optical depth as an indicator of drought-driven tree mortality. *Remote Sensing of Environment*, *227*, 125–136. https://doi.org/10.1016/j.rse.2019.03.026

Rodell, M., Houser, P. R., Jambor, U., Gottschalck, J., Mitchell, K., Meng, C.-J., et al. (2004). The global land data assimilation system. [Dataset]. Bulletin of the American Meteorological Society, *85*(3), 381–394. https://doi.org/10.1175/BAMS-85-3-381

Rogers, B. M., Solvik, K., Hogg, E. H., Ju, J., Masek, J. G., Michaelian, M., et al. (2018). Detecting early warning signals of tree mortality in boreal North America using multiscale satellite data. *Global Change Biology*, *24*(6), 2284–2304. https://doi.org/10.1111/gcb.14107

Scheff, J., & Frierson, D. M. W. (2015). Terrestrial aridity and its response to greenhouse warming across CMIP5 climate models. *Journal of Climate*, *28*(14), 5583–5600. https://doi.org/10.1175/jcli-d-14-00480.1

Scholze, M., Knorr, W., Arnell, N. W., & Prentice, I. C. (2006). A climate-change risk analysis for world ecosystems. *Proceedings of the National Academy of Sciences*, *103*(35), 13116–13120. https://doi.org/10.1073/pnas.0601816103

Senf, C., Buras, A., Zang, C. S., Rammig, A., & Seidl, R. (2020). Excess forest mortality is consistently linked to drought across Europe. *Nature Communications*, *11*(1), 6200. https://doi.org/10.1038/s41467-020-19924-1

Sitch, S., Huntingford, C., Gendney, N., Levy, P. E., Lomas, M., Piao, S. L., et al. (2008). Evaluation of the terrestrial carbon cycle, future plant geography and climate-carbon cycle feedbacks using five Dynamic Global Vegetation Models (DGVMs). *Global Change Biology*, *14*(9), 2015–2039. https://doi.org/10.1111/j.1365-2486.2008.01626.x

Song, X., Hansen, M. C., Stehman, S. V., Potapov, P. V., Tyukavina, A., Vermote, E. F., & Townshend, J. R. (2018). Global land change from 1982 to 2016. *Nature*, *560*(7720), 639–643. https://doi.org/10.1038/s41586-018-0411-9

Splechtna, B. E., Gratzer, G., & Black, B. A. (2005). Disturbance history of a European old-growth mixed-species forest—A spatial dendro-ecological analysis. *Journal of Vegetation Science*, *16*(5), 511–522. https://doi.org/10.1111/j.1654-1103.2005.tb02391.x

Swann, A. L. S., Hoffman, F. M., Koven, C. D., & Randerson, J. T. (2016). Plant responses to increasing CO_2 reduce estimates of climate impacts on drought severity. *Proceedings of the National Academy of Sciences*, *113*(36), 10019–10024. https://doi.org/10.1073/pnas.1604581113

Touma, D., Ashfaq, M., Nayak, M. A., Kao, S.-C., & Diffenbaugh, N. S. (2015). A multi-model and multi-index evaluation of drought characteristics in the 21st century. *Journal of Hydrology*, *526*, 196–207. https://doi.org/10.1016/j.jhydrol.2014.12.011

23284277, 2024, 1, Downloaded from https://agupubs.onlinelibrary.wiley.com/doi/10.1029/2023EF003705 by Cochrane France, Wiley Online Library on [11/01/2024]. See the Terms and Conditions (https://onlinelibrary.wiley.com/terms-and-conditions) on Wiley Online Library for rules of use; OA articles are governed by the applicable Creative Commons License

Trenberth, K. E., Dai, A., van der Schrier, G., Jones, P. D., Barichivich, J., Briffa, K. R., & Sheffield, J. (2014). Global warming and changes in drought. *Nature Climate Change*, *4*(1), 17–22. https://doi.org/10.1038/nclimate2067

Unal, I. (2017). Defining an optimal cut-point value in ROC analysis: An alternative approach. *Computational and Mathematical Methods in Medicine*, *2017*, 3762651–3762714. https://doi.org/10.1155/2017/3762651

Van Mantgem, P. J., Stephenson, N. L., Byrne, J. C., Daniels, L. D., Franklin, J. F., Fulé, P. Z., et al. (2009). Widespread increase of tree mortality rates in the western United States. *Science*, *323*(5913), 521–524. https://doi.org/10.1126/science.1165000

Verbesselt, J., Umlauf, N., Hirota, M., Holmgren, M., Van Nes, E. H., Herold, M., et al. (2016). Remotely sensed resilience of tropical forests. *Nature Climate Change*, *6*(11), 1028–1031. https://doi.org/10.1038/nclimate3108

Vicente-Serrano, S. M., Beguería, S., López-Moreno, J. I., Angulo, M., & El Kenawy, A. (2010). A new global 0.5° gridded dataset (1901–2006) of a multiscalar drought index: Comparison with current drought index datasets based on the Palmer Drought Severity Index [Dataset]. Journal of Hydrometeorology, *11*(4), 1033–1043. https://doi.org/10.1175/2010JHM1224.1

Williams, A. P., Cook, E. R., Smerdon, J. E., Cook, B. I., Abatzoglou, J. T., Bolles, K., et al. (2020). Large contribution from anthropogenic warming to an emerging North American megadrought. *Science*, *368*(6488), 314–318. https://doi.org/10.1126/science.aaz9600

Williams, P. A., Allen, C. D., Macalady, A. K., Griffin, D., Woodhouse, C. A., Meko, D. M., et al. (2013). Temperature as a potent driver of regional forest drought stress and tree mortality. *Nature Climate Change*, *3*(3), 292–297. https://doi.org/10.1038/nclimate1693

Wu, X., Liu, H., He, L., Qi, Z., Anenkhonov, O. A., Korolyuk, A. Y., et al. (2014). Stand-total tree-ring measurements and forest inventory documented climate-induced forest dynamics in the semi-arid Altai Mountains. *Ecological Indicators*, *36*, 231–241. https://doi.org/10.1016/j.ecolind.2013.07.005

Xu, C. (2023). Enhanced drought exposure increasingly threatens more forests than observed [Dataset]. figshare. https://doi.org/10.6084/m9.figshare.23731443.v1

Yang, Y., Roderick, M. L., Zhang, S., McVicar, T. R., & Donohue, R. J. (2019). Hydrologic implications of vegetation response to elevated CO_2 in climate projections. *Nature Climate Change*, *9*(1), 44–48. https://doi.org/10.1038/s41558-018-0361-0

Zhang, Y., Keenan, T. F., & Zhou, S. (2021). Exacerbated drought impacts on global ecosystems due to structural overshoot. *Nature Ecology & Evolution*, *5*(11), 1490–1498. https://doi.org/10.1038/s41559-021-01551-8

Zhu, Z., Piao, S., Myneni, R. B., Huang, M., Zeng, Z., Canadell, J. G., et al. (2016). Greening of the Earth and its drivers. *Nature Climate Change*, *6*(8), 791–795. https://doi.org/10.1038/nclimate3004

23284277, 2024, 1, Downloaded from https://agupubs.onlinelibrary.wiley.com/doi/10.1029/2023EF003705 by Cochrane France, Wiley Online Library on [11/01/2024]. See the Terms and Conditions (https://onlinelibrary.wiley.com/terms-and-conditions) on Wiley Online Library for rules of use; OA articles are governed by the applicable Creative Commons License